ELSEVIER

Chemical Engineering Journal 79 (2000) 41–52

Chemical Engineering Journal

www.elsevier.com/locate/cej

Phase holdup and gas-to-liquid mass transfer coefficient in magneto stabilized G-L-S airlift fermenter

Z. Al-Qodah [a,*], M. Al-Hassan [b]

[a] *Department of Chemical Engineering, Amman College for Engineering Technology, Al-Balqa Applied University, Marka, P.O. Box 340558, Amman, Jordan*

[b] *Department of Mechanical Engineering, Amman College for Engineering Technology, Al-Balqa Applied University, Marka, P.O. Box 340558, Amman, Jordan*

Received 19 June 1999; received in revised form 4 January 2000; accepted 1 March 2000

Abstract

Phase holdups and gas-to-liquid mass transfer coefficient in a three-phase airlift column with magnetic particles were investigated in the presence of an external transverse magnetic field. Experiments were performed in two modes of operation: magnetizing first and magnetizing last.

Gas holdups in the riser and the bed as well as local gas holdup were measured to examine the effect of both the gas superficial velocity and the magnetic field intensity on these parameters. It was found that gas, liquid and solid holdups showed a strong dependence on the gas superficial velocity and the magnetic field intensity. In addition, mass transfer coefficient was determined by the dynamic gassing-in method, and found to increase as gas velocity and magnetic field intensity increase. Correlation equations relating ε_{gr}, ε_{gb}, ε and $K_L a$ to U_g and B in the two modes of operations were proposed.

Keywords: Magnetic stabilization; Three-phase airlift reactor; Magnetically stabilized beds; Phase holdups; Local gas holdup; Mass transfer

1. Introduction

In recent years, three-phase G-L-S airlift reactors have emerged as one of the most promising devices for three-phase operations in the chemical and biochemical industries. These contactors are considered as an alternative of three-phase G-L-S fluidized bed reactors in the search for an efficient mixing among the phases combined with high liquid circulation, in the absence of mechanical agitation [1,2]. Typically, external loop airlift reactor consists of a riser and a downcomer column. The injection of air into the bottom of the riser aerates its contents. The resulting difference in the gas holdup between the gas sparged riser and the downcomer leads to a difference in the bulk densities of the fluids in the two arms. As a result, an induced liquid circulation between the riser and the downcomer through the connecting side arms is set up [3]. The volumetric gas holdup in airlift reactors is an important hydrodynamic parameter, as a relatively large gas holdup in the riser relative to the downcomer increases the liquid circulation [4].

However, it has been recognized that airlift reactors suffer from several drawbacks. Firstly, the gas liquid mass transfer coefficient in airlift is lower than that of conventional bubble columns and three-phase fluidized beds. This behavior is attributed to the possible occurrence of large gas bubbles in the three-phase region, as a result of the large gas superficial velocity needed to fluidize the solid phase [1,5]. Secondly, the flowing gas, in excess of that needed for minimum fluidization, collects as slugs or large bubbles. These slugs result in poor contacting among the phases. This gross bypassing may also cause back mixing of the catalyst phase. Therefore, improvements in the performance of the airlift reactors via reducing the volume of the gas bubbles are needed. These improvements can be achieved by employing a static or motionless mixer in the riser [6] or by applying the principle of magnetic stabilization [7,8].

The application of a magnetic field to a fluidized bed with ferromagnetic particles imposes constraints upon the hydrodynamics not experienced in conventional fluidized systems. A magnetic field changes the bed structure and then changes the bed flow regimes. In addition, a magnetic field with sufficient intensity can eliminate solid mixing and solid movements. Consequently, it suppresses bubble coalescence or enhances bubble disintegration. Therefore, it is expected

* Corresponding author. Tel.: +962-6-487-4545; fax: +962-6-489-4292.
E-mail address: zalqodah@hotmail.com (Z. Al-Qodah)

1385-8947/00/$ – see front matter
PII: S1385-8947(00)00142-X

that both the residence time distribution of the gas bubbles and the radial profile of the gas holdup in a fluidized bed be affected by application of a magnetic field [9].

Kirko and Filipov [10] reported the first observations of the influence of a uniform axial magnetic field on the dynamics of liquid fluidized bed of ferromagnetic particles. Subsequently, Nekrasov and Chekin [11] investigated the behavior of gas fluidized solids in the presence of a transverse magnetic field. Rosensweig [7,12] showed by modeling and experiments that the magnetically fluidized bed provides a unique new means of fluid-solid contacting. According to the researchers, this new reactor combines the best characteristics of both the fluidized and the packed beds. After that there have been a large number of published articles describing the principle of magnetic stabilization as a new approach for modifying the behavior of fluidized beds for ideal conditions. These investigations have recently been reviewed by Liu et al. [13].

It is evident from the published literature that three-phase magnetically stabilized systems have received little attention compared to two-phase systems. Sada et al. [14] applied an axial magnetic field to a three-phase fluidized bed to keep magnetite containing beads in the column over a wide range of fluid velocities. Hu and Wu [15] and Al-Qodah [8] studied the characteristics of three-phase fluidized beds in the presence of an axial and a transverse magnetic field, respectively. They described the fluidization patterns in these systems, and reported on the effect of magnetic field intensity on the bed expansion and gas holdup in addition to other hydrodynamic parameters. Kwauk et al. [16], who studied the behavior of three-phase fluidized beds in an axial magnetic field, reported some empirical equations regarding bubble disintegration conditions. Recently, Thompson and Worden [17] have studied phase holdups, liquid dispersion, and gas-to-liquid mass transfer characteristics in a three-phase fluidized bed utilizing an axial magnetic field. They found that gas holdup decreases and $K_L a$ remains the same or decreases as the magnetic field increases.

Many studies have appeared during the last two decades trying to exploit the advantages of magnetically stabilized systems in some chemical and biochemical processes in addition to some separation techniques [8,18–20]. Recently, Ivanova et al. [21] studied the performance of magnetically stabilized bed reactor with immobilized yeast cells. According to these researchers, higher ethanol concentration and ethanol productivity were reached. Subsequently, Colin et al. [22] applied the magnetic field to an enzyme reactor. They found that the overall mass transfer rate increased from 15 to 47 mole/m^3 s as the magnetic field intensity increased from 0 to 38 mT.

In a more recent study, and as an extension to the magnetic stabilization phenomena, Al-Qodah [23] has studied the effect of magnetic field intensity on some hydrodynamic parameters of three-phase airlift reactor such as flow regimes, bed expansion, minimum fluidization velocity, and liquid circulation velocity. It was found that the bed flow regimes and expansion behavior in magnetically stabilized columns are similar to those in magnetically stabilized three-phase beds, in spite of the high gas velocities used in the former case.

Phase holdup and mass transfer characteristics in magnetic airlift reactors, have not been studied so far. This study aims at investigating the effect of magnetic field intensity on the phase holdups and mass transfer coefficient in a three-phase airlift column utilizing a transverse magnetic field.

2. Experimental

2.1. Experimental setup and materials

A schematic diagram of the experimental setup is shown in Fig. 1. The external loop three-phase column is made of transparent Plexiglas. It consists of a riser tube (i.d. 0.054 m)

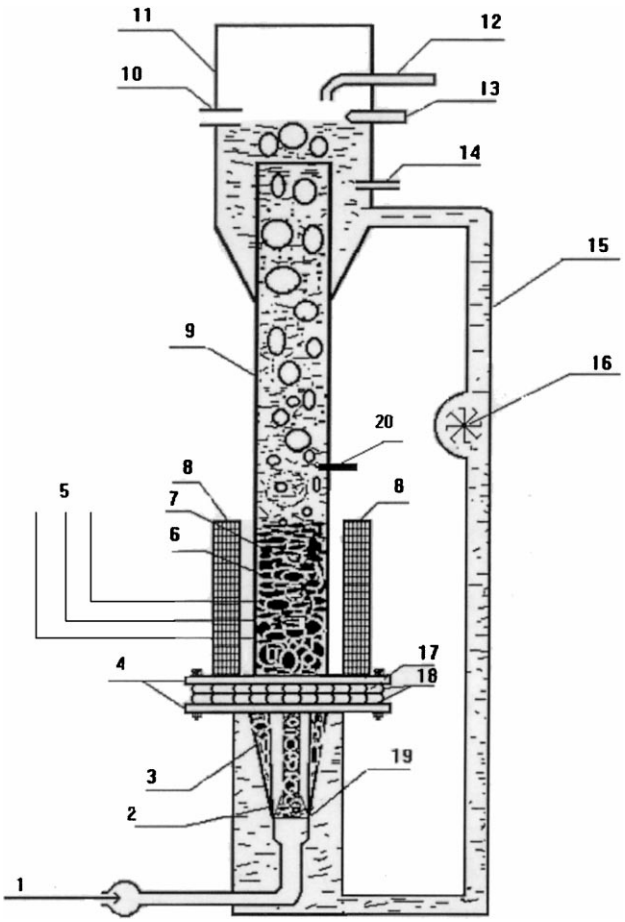

Fig. 1. Schematic diagram of external loop G-L-S airlift reactor utilizing a transverse magnetic field: (1) gas inlet; (2) circulating liquid inlet; (3) polyethylene particle; (4) flanges; (5) pressure taps; (6) magnetic particles; (7) gas holdup probe; (8) magnetic system; (9) riser; (10) overflow tube; (11) degassing section; (12) makeup water inlet; (13) level controller electrode; (14) oxygen electrode; (15) downcomer; (16) photocell turbine; (17) supporting grid; (18) cascade; (19) gas distributor; (20) oxygen electrode.

and a downcomer tube (i.d. 0.018 m). The height of the riser and downcomer, H_r, is 0.75 m and they are 0.15 m apart. Water and air are used as the liquid and gas phases, respectively. Air is fed to the riser from a compressor. A pressure regulator and a needle valve are mounted on the air feed line to adjust gas flow in each experiment. Pressure taps that are connected to water manometers are axially spaced at 0.02 m intervals on the riser wall. These taps were used to measure the static pressure gradients along the riser.

The degassing section consists of transparent cylinder (i.d. 0.2 m) of 0.2 m height and is open to the atmosphere. This part is carefully designed in order to improve the degassing process in such a way that it prevents recirculation of the fine gas bubbles through the downcomer. A perforated non-magnetic, stainless steel grid of 0.0003 m pore diameter is mounted on the base of the riser to support the solid phase and distribute the fluids.

In three-phase airlift reactors, the density difference between the riser and the downcomer is relatively low owing to the presence of the dense solid phase in the riser. For this reason, the air is injected through a sintered glass distributor with a nominal pore size of 50 μm located at 0.04 m below the supporting grid. The bottom end of the downcomer is extended 0.1 m below the distributor. The distributor has a conical shape. Six channels (i.d. 0.008 m) are furnished from its wall up to the supporting grid as a path for the circulated water. This design is used to evenly distribute the gas phase over the whole cross sectional area of the riser. In addition, it prevents the gas phase from entering the downcomer.

The magnetic system is made up of a mild steel core and 1500 coils made of a copper wire of 9×10^{-4} m diameter. The core consists of 180 painted cast steel sheets with 9×10^{-4} m thickness. The cast steel sheets are formed as shown in Fig. 2, in order to house the riser. The net height of the magnetic system is 0.2 m. The dc current can be varied from 0 to 2.5 A, and the maximum magnetic field intensity is about 80 mT. Such a design of the magnetic system has not been cited in the literature before. It produces concentrated and homogeneous magnetic field as indicated by the Hall probe. In addition, it has the advantage of minimizing the electrical energy losses in the form of heat when compared to electromagnets made of solenoids only. The evidence of this fact is that the temperature of the magnetic system does not rise above 40°C for 1 h of continuous operation.

The magnetic particles were prepared in the same manner as described before by Al-Qodah et al. [24]. Their characteristics are shown in Table 1. The magnetic particles consist of a ferromagnetic core of magnetite (Fe_3O_4) covered by a stable layer of activated carbon or zeolite by using epoxy resin as an adhesive. These particles are normally fluidized in the absence of the magnetic field and they are considered as non-porous particles that show good adhesion properties for cell or enzyme immobilization. The activated carbon and zeolite magnetic particles have black and green colors, respectively. These colors facilitate visual observations. The results of this study were obtained by using activated carbon magnetic particles of 1.1 mm diameter.

2.2. Procedure

The initial height of the bed, H_{bo}, is 0.1 m. A scale located on the riser wall was used to measure the bed height in addition to the method of static pressure profiles up the entire height of the riser. The bed height is taken as the point at which a sudden change in the slope of the pressure profile is observed. A level controller is used to maintain a constant liquid level in the degassing section. A variable area meter (Platon, UK) is used to measure the gas flow rate.

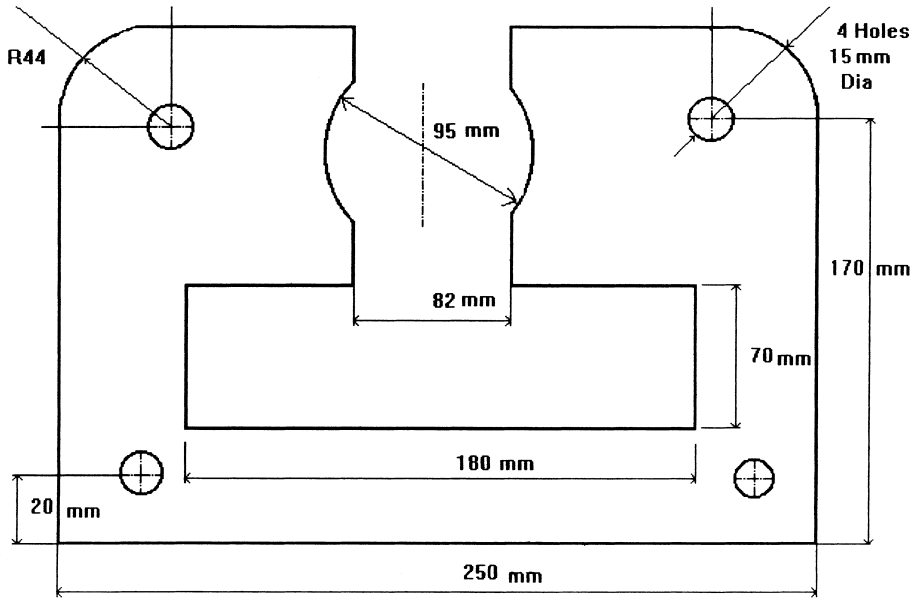

Fig. 2. Schematic diagram of a sheet of the magnetic system.

Table 1
Characteristics of the magnetic particles used in this study

Material used to cover magnetite	ρ_b (kg/m^3)	ρ_s (kg/m^3)	Shape factor	d_p (mm)	U_{mfo} (m/s)	B_s (mT)	Color	Porosity, ε_o	C_p (J/kg)
Activated carbon 1	1750	3020	0.9	0.9	0.574	590	Black	0.42	362
Activated carbon 2	1905	3230	0.9	1.0	0.690	590	Black	0.41	370
Zeolite	2100	3500	0.8	1.1	0.803	590	Green	0.40	478

The riser gas holdup, ε_{gr}, is determined by collecting the overflowing water from the degassing section which floods after the injection of the gas phase from the distributor. This method is found to be suitable for measuring the riser gas holdup in both modes of operation, because in magnetizing first mode the gas holdup increases as the gas velocity increases, and in magnetizing last mode, gas holdup increases as the magnetic field intensity increase.

The overall holdups in the three-phase region are determined directly from the measurement of the particles weight within the bed. The following relationships hold for phase holdups: the initial solid holdup, ε_{so}, and solid holdup after bed expansion, ϵ_s, are given by

$$\varepsilon_{so} = \frac{W/\rho_s}{AH_{bo}} \tag{1}$$

$$\varepsilon_s = 1 - \left(\frac{H_{bo}}{H_b}\right)\varepsilon_{so} \tag{2}$$

The following equation holds for the bed porosity, ε:

$$\varepsilon = 1 - \varepsilon_s \tag{3}$$

The mean gas holdup in the three-phase bed is determined from the following equation:

$$\varepsilon_{gb} = \varepsilon_{gr} - \varepsilon_a \tag{4}$$

where $\varepsilon_a = \dfrac{H_a - H_w}{H_a}$

Liquid holdup in the three-phase bed, ε_l, is calculated from the following equation:

$$\varepsilon_l = 1 - \varepsilon_s - \varepsilon_{gb} \tag{5}$$

Liquid circulation velocity, $U_{lc,}$ is measured using a photocell. The measuring circuit of this device is shown in Fig. 3. It consists of a light source detector and a plastic turbine mounted vertically on the middle of the downcomer. The plastic turbine rotates at a rate proportional to the liquid circulation velocity. Thus, its blades cut the light beam and affect the reading of the light detector. The output of the photocell is calibrated with a variable area rotameter.

Local gas holdup, ε_{gl}, is measured using an electroresistivity probe. The measuring circuit of this probe is shown in Fig. 4. The probe is contained in a metallic cover (i.d. 0.004 m) except for a distance of 0.003 m from the tip. The annular space between the electrode sensitive tip and the metallic cover is filled with epoxy resin as an insulator. The sensitive tip, which is exposed to the three-phase bed, has a diameter of 0.02 mm and it is cut to have a flat surface that makes 45° with the riser axis. A seal is provided between the wires and the end of the metallic cover. The probe is mounted at a height of 0.06 m above the supporting grid using a silicon stopper as seal. The electrode is movable and could be positioned at any point in the radial direction of the riser. A DC amplifier adjusts the output of the probe to give a voltage drop ranging from 0 to 1 V when the circuit at the tip of the probe is opened and closed by

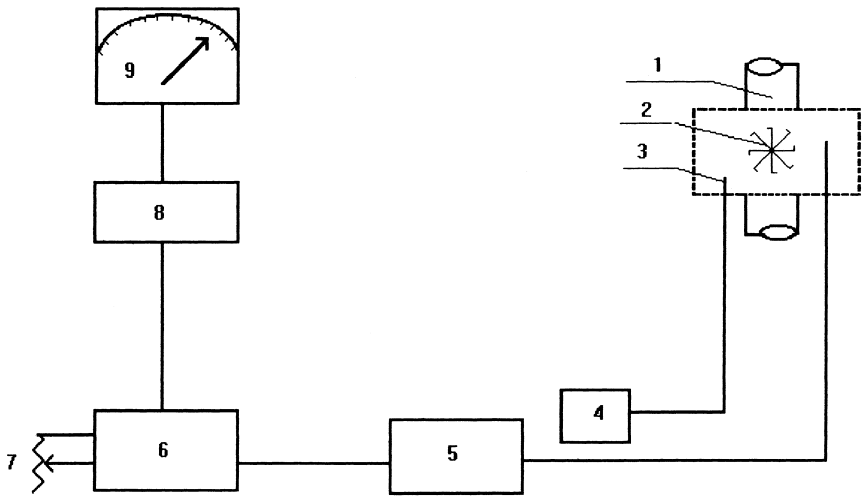

Fig. 3. Electrical circuit of the photocell: (1) downcomer; (2) turbine; (3) signal; (4) DC source; (5) primary amplifier; (6) counter; (7) sensitivity knob; (8) AC to DC converter; (9) readout.

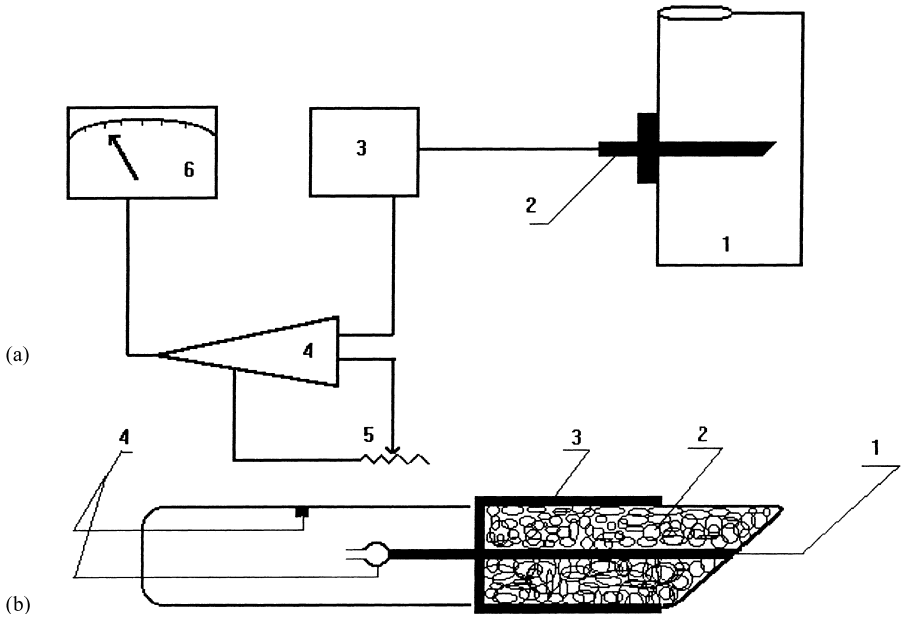

Fig. 4. Electrical circuit of electroresistivity probe. (a): (1) riser; (2) probe; (3) amplifier; (4) operative amplifier; (5) calibration; (6) readout; (b): (1) Electrode sensitive tip; (2) epoxy resin; (3) metallic cover; wires to the measuring circuit.

the bubble and liquid phase, respectively. The output from the electrode is transformed into a digital readout. A Hall probe (Leybolo-Heraeus, Germany) is used to measure the magnetic field intensity.

The overall volumetric mass transfer coefficient, $K_L a$, in the riser is determined by means of the dynamic gassing-in method [17,25,26]. The dissolved oxygen is first removed from the reactor by sparging nitrogen gas until the dissolved oxygen concentration falls to 0–5%, at a nitrogen superficial velocity of 0.025 m/s. After that the nitrogen flow is stopped and the air flow was started. The change of the dissolved oxygen concentration in the riser is measured with fast oxygen probe (Gallen Kamp, UK) whose probe is inserted through the riser wall at a height of 0.23 m above the supporting grid. The probe time constant is 0.84 s for a sudden probe transfer from N_2 to O_2 saturated water. The output signals from the probe are processed in a module system, which changes the signal to percent saturation as a digital readout. Each run is stopped when the dissolved oxygen concentration reached saturation.

The oxygen mass transfer balance is the given by the following equation:

$$\frac{dC_l}{dt} = K_L a(C_l^* - C_l) \quad (6)$$

When $K_L a$ is considered to be independent of time, integration of Eq. (6) with C_l=0 at t=0 gives

$$C_l(t) = C_l^* \left(1 - \mathrm{Exp}\left(-\frac{K_L a}{t}\right)\right) \quad (7)$$

The overall volumetric mass transfer coefficient, $K_L a$, is determined from the slope of the straight line obtained from a plot of $\ln(C_l^* - C_l)$ against time. This method of evaluating $K_L a$ is applicable when assuming a well-mixed liquid phase, a constant gas concentration along the riser height and a fast response of the oxygen electrode to a change in the dissolved oxygen concentration. These assumptions are in good agreement with the hydrodynamic behavior of the present reactor. Liquid circulation velocity, $U_{lc,}$ is sufficient to cause good mixing to satisfy the first assumption, i.e. U_{lc} values cover the ranges from 0.005 to 0.018 m/s. The low solubility of oxygen in the liquid phase and the fast response of oxygen electrode are expected to fulfill the second and the third assumption, respectively.

2.3. Experiments in this study were conducted in two modes

1. 'Magnetizing first' which means that the magnetic field is turned at a desired value and applied to a static bed. After that the fluid velocity is increased. In this mode of operation and before starting each experiment, the bed is fluidized in the absence of the magnetic field for 3 min, followed by a slow decrease of the gas flow rate down until the formation of the initial packed bed. This procedure limited the residual effects of past experiments at high magnetic fields.
2. 'Magnetizing last' which means that the bed is first fluidized, then the magnetic field intensity is gradually increased while keeping the gas velocity at a constant value.

3. Results and discussion

3.1. Riser gas holdup

Fig. 5 shows the average riser gas holdup, ε_{gr}, as a function of gas superficial velocity, U_g, at magnetic field intensities of 0, 26 and 76 mT (magnetizing first mode). Two important points are evident in this figure. First, the riser gas holdup, ε_{gr} increases as the superficial gas velocity, U_g, increases. Second, the rate at which ε_{gr} increases, depends on U_g and the magnetic field intensity. For example, this rate increases at low gas velocities, i.e. $U_g < 0.03$ m/s and decreases at relatively higher gas velocities as the magnetic field intensity increases. Fig. 5 shows that when the gas velocity increases from 0.02 to 0.21 m/s, the riser gas holdup increases 311, 227, and 172% at magnetic field intensities of 0, 26, and 76 mT, respectively.

In order to understand this behavior of the riser gas holdup under the combined effect of both the gas superficial velocity and the magnetic field intensity, it is necessary to describe the effects of these parameters on the bed flow regime and expansion characteristics in the two modes of operation. It is observed that when the gas superficial velocity is increased while maintaining constant magnetic field intensity, the bed starts to change its structure by a process of slow and regular expansion. Furthermore, agglomeration of the magnetic particles into aggregates or strings oriented horizontally with the field lines was clearly seen before the onset of the fluidized bed regime, i.e. in the magnetically stabilized regime. These stagnant strings or chains of particles are able to prevent coalescence of the small gas bubbles especially at relatively high magnetic field intensities. As a result, the gas bubbles rising velocity remains constant leading to an increase in the bubble residence time in the bed and consequently increases the gas holdup. The diameter of the largest bubble leaving the stabilized bed is about 0.003 m.

After the destruction of the stabilized bed at a fluid velocity beyond the minimum fluidization velocity, a fluidized bed of aggregates of particles exists. In this regime solid mixing starts and its intensity increases when increasing the gas superficial velocity. In addition, bubble coalescence occurs and the diameter of the bubbles leaving the bed reaches 0.01 m. In this case the bubble rising velocity increases. As a result the effect of the magnetic field intensity on the riser gas holdup in the fluidized regime is not significant. It is evident from Fig. 5 that at gas velocities beyond 0.2 m/s, the values of the riser gas holdup are independent on the magnetic field intensity.

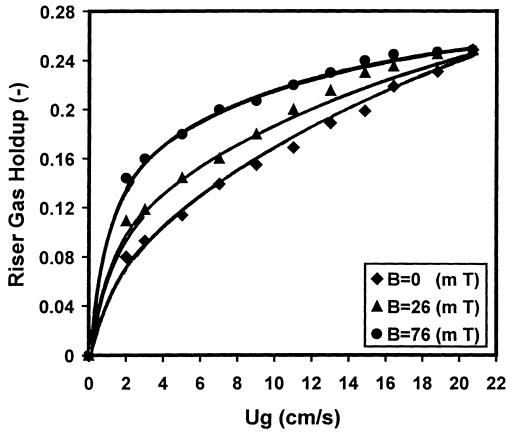

Fig. 5. Effect of gas velocity on ε_{gr} for three magnetic field intensities (magnetization first mode).

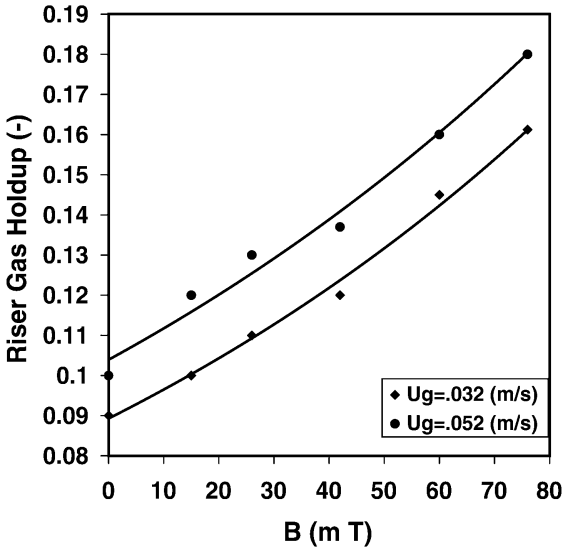

Fig. 6. Effect of magnetic field intensity on ε_{gr} at two different gas velocities (magnetizing last mode).

Fig. 6 shows the effect of magnetic field intensity, B, on the riser gas holdup, ε_{gr}, at gas velocities of 0.032 and 0.052 m (magnetizing last mode). It can be seen that as the magnetic field intensity changes from 0 to 70 mT, the riser gas holdup increases from 0.09 to 0.16 and from 0.1 to 0.18 at gas velocities of 0.032 and 0.052 m/s, respectively. In addition, the effect of the magnetic field intensity on the riser gas holdup in this mode of operation resembles that in the magnetizing first mode. The bed in both modes undergoes expansion as a result of the simultaneous action of both the arrangements of the aggregates in the direction of the field lines and the momentum of the flowing fluids.

The riser gas holdup data are correlated in terms of the gas superficial velocity and the magnetic field intensity since the other parameters are maintained constants. The computer program for curve fitting 'Origin' obtains the empirical relation given below:

$$\varepsilon_{gr} = 0.45269 U_g^{0.4727} \exp 0.0077 B \quad (8)$$

In this correlation the range of variables covers U_g from 0.02 to 0.20 m/s and B from 5 to 76 mT. At these conditions an expanded stabilized bed exists. Below these values the bed is packed with very low liquid circulation rate. In addition, if $B < 5$ mT, the resulting magnetic cohesion forces among

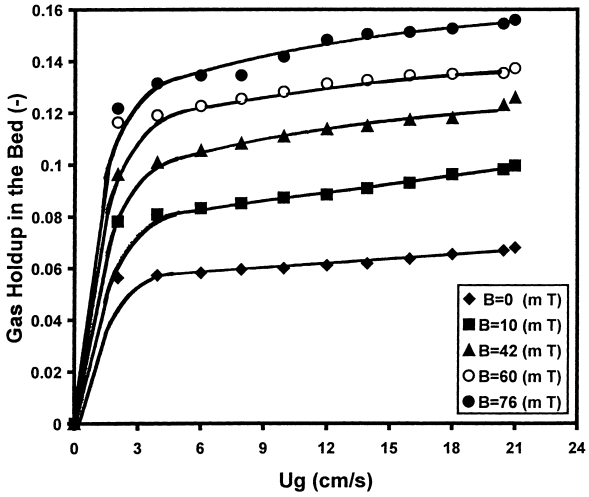

Fig. 7. Effect of the gas velocity on ε_{gb} at several magnetic field intensities (magnetizing first mode).

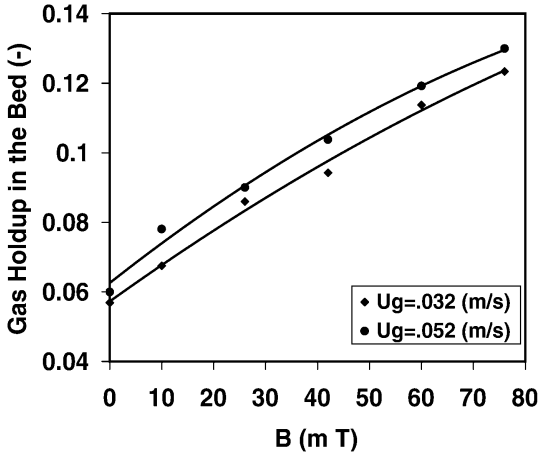

Fig. 8. Effect of magnetic field intensity on ε_{gb} at two gas velocities (magnetizing last mode).

the particles in the bed are weak and do not influence the bed hydrodynamics. The standard error of estimate is 0.071.

3.2. Bed gas holdup

Fig. 7 shows the mean gas holdup data in the three-phase bed, ε_{gb}, as a function of gas superficial velocity at magnetic field intensities of 0, 10, 42, 60, and 76 mT (magnetizing first mode). It is evident that ε_{gb} increases when increasing the gas velocity. In addition, the rate of increase is higher at low gas velocities, after the injection of the gas phase in the riser, than it is at high gas velocities. For example, at a magnetic field intensity of 42 mT, ε_{gb} increases from 0 to 9.6% and from 10.1 to 10.8% as the gas velocity increases from 0 to 0.02 and from 0.06 to 0.08 m/s, respectively. Furthermore, it is clearly seen that for the same gas velocity, ε_{gb} increases as the magnetic field intensity increases. This behavior is attributed to the fact that the magnetic field constrains particle movement, hence increasing resistance to gas flow. Because the bubble rise velocity is reduced, the gas holdup increases. Fig. 7 shows that at any gas velocity, ε_{gb} increases more than twice as the magnetic field intensity increases from 0 to 76 mT.

The effect of increasing the magnetic field intensity on ε_{gb} at gas velocities of 0.032 and 0.052 m/s (magnetizing last mode) is shown in Fig. 8. It is evident that at a gas velocity of 0.032 m/s, ε_{gb} increases from 5.7 to 12.5% as the magnetic field intensity increases from 0 to 76 mT. The reason for this behavior is attributed again to the effect of the magnetic field on the bed structure and porosity as mentioned earlier. This behavior of increasing ε_{gb} as a result of increasing B in a magnetically stabilized bed utilizing a transverse magnetic field is the opposite of the behavior of ε_{gb} in a magnetically stabilized utilizing an axial magnetic field. In the latter case bed contraction occurs, consequently ε_{gb} decreases when increasing the magnetic field intensity [7,15,17].

The following correlation relates ε_{gb} to the gas superficial velocity and the magnetic field intensity:

$$\varepsilon_{gb} = (0.0404 + 0.033U_g)B^{0.229} \quad (9)$$

In this correlation the range of variables is the same as in Eq. (8) and the standard error of estimate is 0.051.

The behavior of ε_{gb} in three-phase magneto airlift columns resembles that in three-phase magneto fluidized beds, although its values in the former are higher, due to the relatively high gas velocities used.

3.3. Local gas holdup

Changing the radial location of the electroresistivity probe systematically produces radial profiles of the local gas holdup, ε_{gl}, at different gas superficial velocities and different magnetic field intensities. Fig. 9 shows the results of local gas holdup measurements at constant gas superficial velocity of 0.052 m/s and three different magnetic

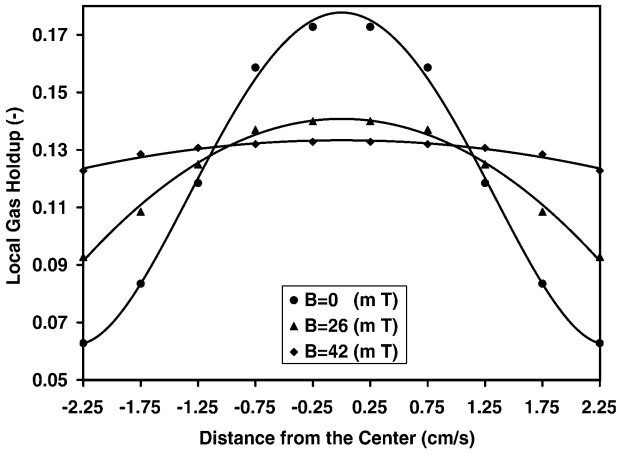

Fig. 9. Effect of magnetic field intensity on the local gas holdup at a gas superficial velocity of 0.052 m/s (magnetizing first mode).

field intensities of 0, 26, and 42 mT. The bed flow regimes corresponding to these magnetic intensities are fluidized, stabilized, and frozen bed regimes, respectively. It can be seen in Fig. 9 that ε_{gl} at the column wall increases from 33 to 67% and finally to 94% of its value at the column axis as the applied magnetic field intensity changes from 0 to 26 to 42 mT, respectively. This means that while increasing the magnetic field intensity, elimination of the local gas holdup gradients in the radial direction occurs. Consequently, this leads to the elimination of the broad residence time distribution of the gas phase and the reduction of back mixing in the liquid phase. The elimination of the local gas holdup gradient in the radial direction is considered as one of the major advantages of magnetic field stabilization. This behavior is very useful in the case of modeling of mass transfer processes in such systems, i.e. the assumptions of the absence of radial gradients in the gas phase and the absence of back mixing in the liquid phase are valid.

Integration of the local gas holdup for the whole bed volume gives an average of 92% of the value of the manometrically obtained average bed gas holdup. This result indicates that the probe is able to detect the majority of the gas bubbles existing in the riser. The other 8% of the gas bubbles could be considered as very small, and cannot be detected by the probe. Thus, local gas holdup measured by the electroresistivity probe could be used to evaluate the radial profiles of the local gas holdup, and give a good approximation of the bed mean gas holdup. However, the absolute value of the mean gas holdup in the bed could be accurately measured only by the direct manometric method described earlier.

The results obtained in this mode of operation are in agreement with those of Hu and Wu [15], who showed using electroresistivity probe that the radial profile of ε_{gl} decreases when increasing the intensity of an axial magnetic field.

Fig. 10 depicts the effect of three different gas superficial velocities of 0.032, 0.052, and 0.12 m/s on ε_{gl} at a constant magnetic field intensity of 42 mT. It is evident from Fig. 10 that ε_{gl} gradients are not significant at U_g values of 0.032 and 0.052 m/s. The bed in this case is magnetically stabilized since these values of U_g are below the minimum fluidization velocity, U_{mf}, that corresponds to the applied magnetic field intensity of 42 mT, i.e. U_{mf}=0.105 m/s. Beyond the minimum fluidization velocity, the local gas holdup gradient gradually increases as the bed under these conditions is fluidized and is characterized by random motions of the particle strings. In these circumstances the gas phase concentrates near the axis of the riser. For example, it appears from Fig. 10 that at U_g of 0.12 m/s and B of 42 mT, ε_{gl} at the wall is about 64% of its value when it is in the center.

3.4. Bed porosity

The bed porosity, ε, is defined as the fraction of the bed volume occupied by both liquid and gas phases, and as such, is directly proportional to the expanded bed height [27]. Fig. 11 depicts the variations of the bed porosity, ε, with the gas superficial velocity, U_g, at magnetic field intensities of 0, 10, 26, 42, 60, and 76 mT (magnetizing first mode). It can be seen in Fig. 11 that ε increases as the gas velocity increases. The behavior of bed porosity increase depends on both U_g and B. The bed porosity increases at a high rate at relatively low gas velocity, i.e. U_g<0.06 m/s and high magnetic field intensity, i.e. B>26 mT. When the gas velocity exceeds 0.065 m/s at magnetic field intensities of 26, 42, 60, and 76 mT bed porosity increases in a relatively slow rate. This behavior is attributed to the bed structure at these conditions and to the maximum height of the bed, which cannot exceed the height of the magnetic system.

One more phenomenon regarding bed porosity in this mode of operation, is the ability of the applied field to expand the bed before starting the gas flow. This phenomenon can be attributed to two reasons. Firstly, as the initial bed height is shorter than that of the magnetic system, the field lines tend to stretch up the particles to cover the whole height

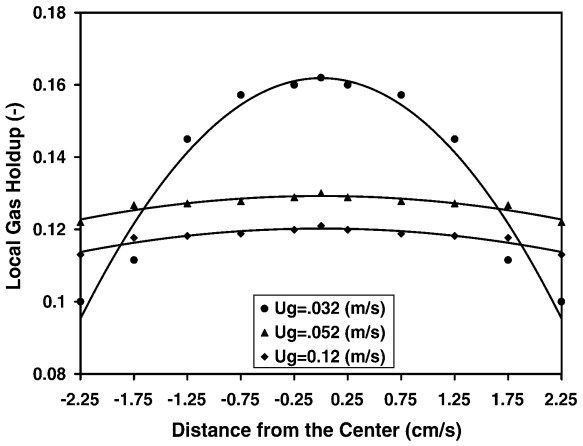

Fig. 10. Effect of gas superficial velocity on the local gas holdup at a magnetic field intensity of 42 mT (magnetizing last mode).

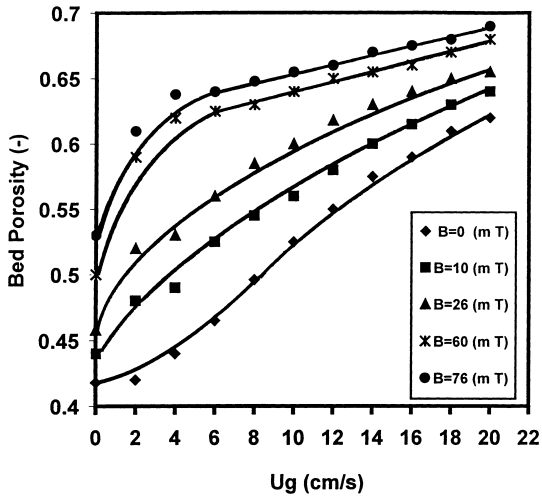

Fig. 11. Effect of the gas velocity on bed porosity, ε, at several magnetic field intensities (magnetizing first mode).

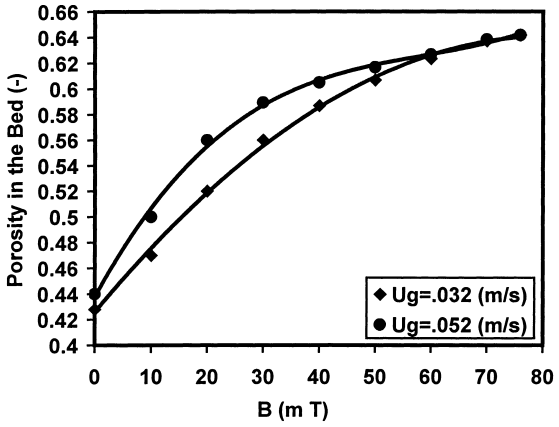

Fig. 12. Effect of magnetic field intensity on bed porosity, ε, at two different gas velocities (magnetizing last mode).

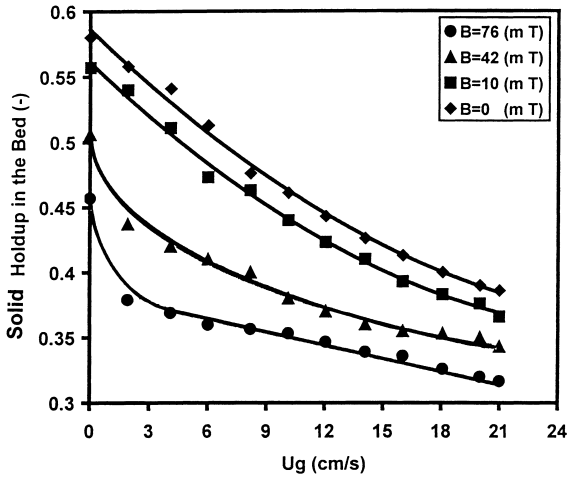

Fig. 13. Effect of gas velocity on solid holdup, ε_s, at several magnetic field intensities (magnetizing first mode).

of the magnetic system. Secondly, the magnetized particles tend to orient themselves horizontally with the field lines. As shown in Fig. 11, the initial bed porosity, i.e. ε at U_g=0 m/s increases from 0.42 to 0.525 as the magnetic field intensity increases from 0 to 76 mT.

Fig. 12 shows the effect of the magnetic field intensity on the bed porosity at gas velocities of 0.032 and 0.052 m/s (magnetizing last mode). It is evident from Fig. 12 that at U_g of 0.052 m/s the fluidized bed porosity increases from 0.44 to a maximum porosity of 0.642 as B increases from 0 to 76 mT. During this expansion process, the magnetic field tends to orient the formed strings horizontally with the field lines, and it suppresses their movements. At relatively high values of B, i.e. B>60 mT, the string movements are completely impeded. At this point a frozen bed is said to exist. In this regime the magnetic particles form a porous and stationary mass.

The bed porosity data are correlated and the following empirical formula is obtained:

$$\varepsilon = 0.6115 U_g^{0.1853} B^{0.1588} \quad (10)$$

The range of variables in this correlation is as in Eq. (8) and the standard error of estimate is 0.045.

It should be noted that bed expansion in this magnetizing last mode of operation represents one of the basic differences between the effect of a transverse and an axial magnetic field where the fluidized bed contracts as the magnetic field intensity increases [7,15]. Although the axial fields provides a greater degree of magnetic stabilization than a transverse field, the latter gives a more uniformed bed structure than the former where channels are easily formed.

Notably, the bed expansion behavior in this mode of operation (i.e. the bed expands as the magnetic field intensity increases), might be an advantage of a transverse magnetic field over an axial magnetic field, where the bed height decreases as the magnetic field intensity increases. Contraction of the fluidized bed results in the formation of channels in the formed aggregated bed [9,15]. Consequently, a transverse magnetic field produces a more uniformed structure of the stabilized bed, than an axial field in which channels are easily formed. However, an axial magnetic field provides a stabilized bed of wider range of the operating gas velocity in magnetizing first mode, i.e. higher U_{mf} value than that in a transverse magnetic field at the same magnetic field intensity [7].

3.5. Solid holdup

Fig. 13 shows the effect of gas superficial velocity on the solid holdup, ε_s, at magnetic field intensities of 0, 10, 42, and 76 mT. It is clear from Fig. 13 that at constant B, the solid holdup decreases rapidly after the injection of the gas phase. Then it decreases at a slower rate with increasing U_g. At a relatively high magnetic field intensity, i.e. B>42 mT, and when U_g exceeds 0.12 m/s, ε_s decreases at approximately constant rate because the bed at these conditions is fluidized and its expansion behavior resembles that of unstabilized bed.

Fig. 14 depicts the variation of ε_s with B at U_g of 0.032 and 0.052 m/s (magnetizing last mode). For example, Fig. 14 showed that at U_g of 0.052 m/s, ε_s decreases from 0.575 to 0.4 as B increases from 0 to 76 mT. This behavior is attributed to the effect of the magnetic field intensity on the bed porosity. It has been mentioned above that as B increases ε increases. Consequently, ε_s decreases as Eq. (3) implies, but at relatively high values of B where a frozen bed exists, B does not affect the solid holdup. By using Eq. (3) and the empirical Eq. (10) the solid holdup can be calculated.

3.6. Liquid holdup

Phase holdup is one of the important hydrodynamic phenomena in three-phase systems. It affects the bed volume and the residence time of the fluid phases. In particular, the liquid phase plays an important role in correlating both heat

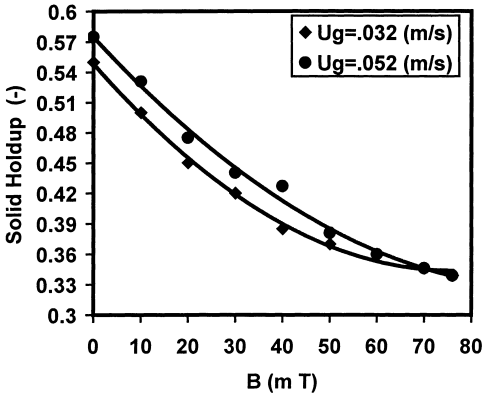

Fig. 14. Effect of magnetic field intensity on solid holdup, ε_s, at two different gas velocities (magnetizing last mode).

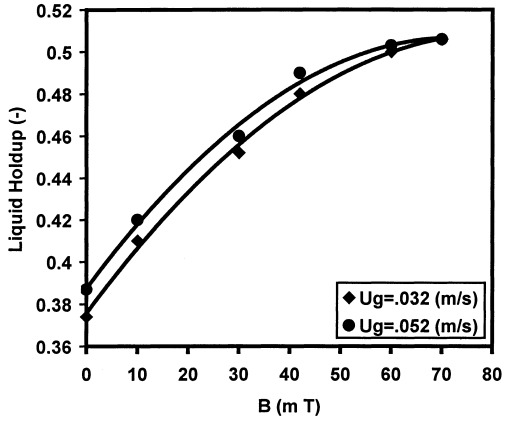

Fig. 16. Effect of magnetic field intensity on liquid holdup, ε_l, at two different gas velocities (magnetizing last mode).

transfer and mass transfer coefficients [28]. For this reason, the effect of gas velocity and magnetic field intensity on liquid holdup, ε_l, is studied.

Fig. 15 shows the effect of gas velocity on the liquid holdup at magnetic field intensities of 0, 10, 42, and 76 mT. It can be seen that ε_l rapidly decreases after the injection of the gas phase when the bed exists in the packed regime, i.e. U_g<0.02 m/s. In the range U_g>0.02 m/s, the bed starts to expand and as a consequence ε_l increases as U_g increases, owing to the gradual increase of the bed porosity.

The variations of liquid holdup with magnetic field intensity at gas velocities of 0.032 and 0.052 m/s are shown in Fig. 16 (magnetizing last mode). At a gas velocity of 0.052 m/s, liquid holdup increases from 0.387 to 0.506 as B increases from 0 to 76 mT owing to the increase of bed porosity.

3.7. Gas-to-liquid mass transfer coefficient

Gas-to-liquid mass transfer coefficient is an important parameter in the overall performance of some three-phase G-L-S systems. The significance of this parameter increases in bioreactors where oxygen is a critical substrate for cell metabolism and for bio-oxidation reactions, owing to the poor solubility of oxygen in aqueous solutions. Enhancement of oxygen transfer to the liquid phase in aerobic bioprocesses is a primary requirement to maintain the activity of the biocatalyst and to increase the rate of the aerobic processes.

Fig. 17 depicts the effect of U_g on the mass transfer coefficient, K_La, at magnetic field intensities of 0, 42, and 70 mT. It can be seen in Fig. 17 that K_La is strongly dependent on U_g in the three-phase airlift contactors. For example, at a magnetic field intensity of 42 mT, K_La increases from 2.0×10^{-2} to 5.75×10^{-2}/s as U_g increases from 0.02 to 0.10 m/s. Fig. 17 shows that the influences of gas flow rate on K_La for a given magnetic field intensity may be represented by a linear equation. In addition, K_La is positively affected by the application of the magnetic field owing to its effect on the gas holdup, bubble sizes and bed height. The magnetic field increases ε_{gb}, and the bed height, H_b,

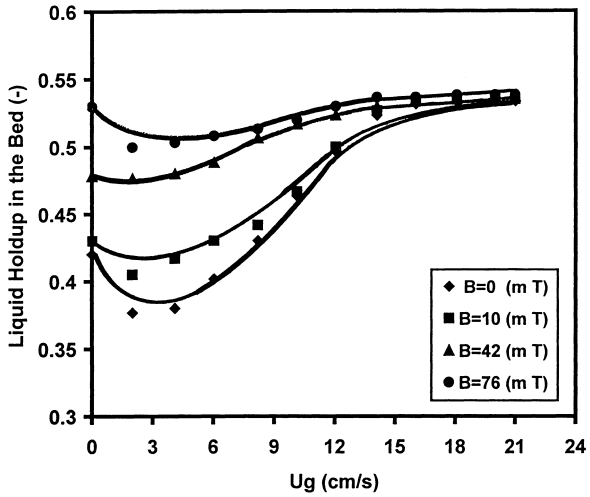

Fig. 15. Effect of gas velocity on the liquid holdup, ε_l, at several magnetic field intensities (magnetizing first mode).

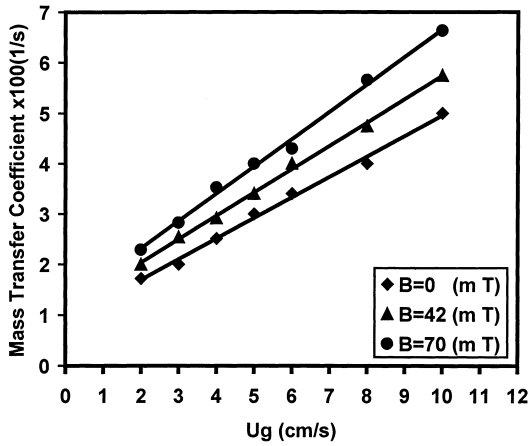

Fig. 17. Effect of gas velocity on K_La, at three different magnetic field intensities (magnetizing first mode).

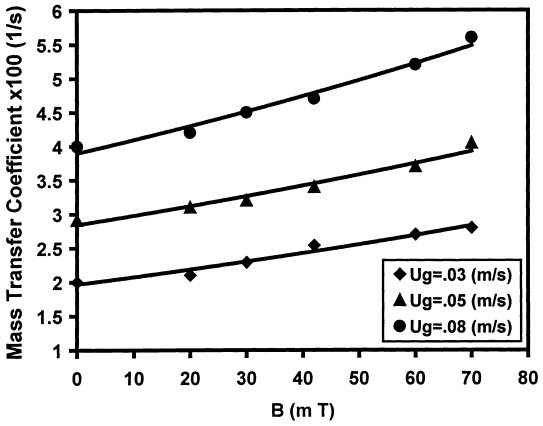

Fig. 18. Effect of magnetic field intensity on $K_L a$, at several gas velocities (magnetizing last mode).

and reduces the bubble sizes. As a result, the magnetic field increases the specific surface area, a, of the bubbles.

Fig. 18 shows the variations of $K_L a$ with B at gas velocities of 0.03, 0.05, and 0.08 m/s (magnetizing last mode). It can be seen that at a gas velocity of 0.05 m/s, $K_L a$ increases from 2.9×10^{-2} to 4.05×10^{-2}/s, i.e. 39% as the magnetic field intensity increases from 0 to 76 mT, due to the same reasons mentioned above. These results are in agreement with those of Colin et al. [22] who found that the magnetic field increases the rate of reaction. In contrast, Thompson and Worden [17] reported that $K_L a$ in a three-phase fluidized bed utilizing an axial magnetic field decreases or remains constant when increasing B.

The mass transfer coefficient data are correlated in terms of U_g and B and the following empirical relation is obtained:

$$K_L a = (0.0095 + 0.37U_g)B^{0.0046} \quad (11)$$

The range of variables in this correlation is the same as in Eq. (8) and the standard error of estimate is 0.052.

4. Conclusions

The experiments carried out, have allowed an assessment of the effect of a uniform, transverse and steady magnetic field on the phase holdups and gas-to-liquid mass transfer coefficient in a three-phase airlift reactor with magnetic particles. The experimental results show significant changes in the behavior of these parameters in magnetized beds over those in conventional systems.

The effects of the intensity of the applied magnetic field and the gas superficial velocity on the riser and bed gas holdups, the local gas holdup, liquid holdup, solid holdup, and the bed porosity are investigated. It is found that ε_{gr}, ε_{gb}, and ε increase when increasing B and U_g while operating in the stabilized regime. In contrast, ε_s, and ε_l decrease under the same conditions. In addition, while the magnetic field tends to eliminate the radial differences in the local gas holdup values, the gas superficial velocity tends to increase these differences. Furthermore, both of U_g and B have a positive effect on the mass transfer coefficient.

The two modes of operation, i.e. magnetizing first and magnetizing last, have not been found to produce significant differences in the phase holdups and mass transfer characteristics. Any difference can be attributed to the formation of radial cracks in the bed at high values of U_g and B in the magnetizing last mode.

Correlation equations for ε_{gr}, ε_{gb}, ε and $K_L a$ as functions of both U_g and B are proposed. These empirical equations show good agreement with the experimental data especially that under conditions where a stabilized bed regime exists.

5. Nomenclature

A	cross-sectional area of the riser (m^2)
B	magnetic field intensity (mT)
C_l	instantaneous oxygen concentration in the liquid phase (kmol/m^3)
C_l^*	oxygen concentration in the liquid phase in equilibrium with the gas phase (kmol/m^3)
d_p	water height in the manometer that corresponds to the static pressure at supporting grid (m)
H_a	riser height–bed height (m)
H_b	bed height(m)
H_{bo}	initial bed height (m)
H_r	riser height (m)
H_w	water height in the manometer corresponding to the static pressure at the bed surface (m)
$K_L a$	gas-to-liquid mass transfer coefficient (/s)
M_s	saturation magnetic intensity (mT)
t	time (s)
U_g	gas superficial velocity (m/s)
U_{lc}	liquid circulation velocity (m/s)
U_{mf}	minimum fluidization velocity (m/s)
U_{mfl}	minimum fluidization velocity with liquid only (m/s)
W	bed weight (kg)
ρ_s	density of the magnetic particles (kg/m^3)
ε	bed porosity, dimensionless
ε_a	gas holdup above the three-phase bed (dimensionless)
ε_{gb}	gas holdup in the bed (dimensionless)
ε_{gl}	local gas holdup in the bed (dimensionless)
ε_{gr}	gas holdup in the riser (dimensionless)
ε_l	liquid holdup (dimensionless)
ε_s	solid holdup (dimensionless)
ε_{so}	initial solid holdup (dimensionless)

References

[1] Y. Kawse, N. Hashiguchi, Gas–liquid mass-transfer in external loop airlift columns with Newtonian and non-Newtonian fluids, Chem. Eng. Sci. 62 (1996) 35–42.

[2] G.H. Schoutens, R.P. Gurl, G.L. Zeilman, K.Ch.A.M. Luyben, N.W.F. Kossen, A comparative study of a fluidized bed reactor and a gas lift loop reactor for IBE process. Part 1. Reactor design and scale down approach, J. Chem. Technol. Biotechnol. 36 (1986) 335–343.
[3] Y. Chisti, B. Halard, M. Moo-Young, Liquid circulation in airlift reactors, Chem. Eng. Sci. 43 (1988) 451–457.
[4] W.J. McManamey, D.A.J. Wase, S. Wase, K. Thayanithy, The influence of gas inlet design on gas hold-up values for water and various solutions in a loop-type air-lift fermenter, J. Chem. Technol. Biotechnol. 343 (1984) 151–164.
[5] R.A. Bello, C.W. Robinson, M. Moo-Young, Gas holdup and overall volumetric oxygen transfer coefficient in airlift contactors, Biotech. Bioeng. 27 (1985) 369–381.
[6] Y. Chesti, M. Kasper, M. Moo-Young, Mass transfer in external loop airlift bioreactors using static mixers, Can. J. Chem. Eng. 68 (1990) 45–50.
[7] R.E. Rosensweig, Fluidization: hydrodynamic stabilization with a magnetic field, Science 204 (1979) 57–60.
[8] Z. Al-Qodah, Performance of a three-phase fluidized bed with immobilized cells in the presence of a transverse magnetic field, Ph.D. Thesis, Sofia University, Chem. Technol., Sofia, Bulgaria, 1991.
[9] P. Genzens, D. Thoenes, Magnetically stabilized fluidization. Part 1. Gas and solid flow, Chem. Eng. Commun. 67 (1988) 217–228.
[10] I.M. Kirko, M.V. Filippov, Standard correlations for a fluidized bed of ferromagnetic particles in a magnetic field, Zn. Tekh. Fiz. 30 (1960) 1081–1088.
[11] Z. Nekrasov, V. Chekin, Effect of an alternating magnetic field on a fluidized bed of ferromagnetic particles, Institute Fizika Latv. 12 (1961) 215–220.
[12] R.E. Rosensweig, Magnetic stabilization of the state of uniform fluidization, Ind. Eng. Chem. Fun. 18 (1981) 261–269.
[13] Y.A. Liu, R.K. Hamby, R.D. Colberg, Fundamental and practical developments of magneto-fluidized beds, Powder Technol. 64 (1991) 3–41.
[14] E. Sada, S. Katoh, M. Shiozawa, T. Fukui magnetically stirred fluidized bed reactor, Biotechnol. Bioeng. 25 (1983) 2285–2292.
[15] T.T. Hu, J.Y. Wu, Study of the characteristics of biological fluidized bed in a magnetic field, Chem. Eng. Res. Dev. 65 (1987) 238–243.
[16] M. Kwauk, X. Ma, F. Ouyang, Y. Wu, D. Weng, L. Cheng, Magneto fluidized G/L/S systems, Chem. Eng. Sci. 47 (1992) 3467–3474.
[17] V.S. Thompson, R.M. Worden, Phase holdup, liquid dispersion, and Gas-to-liquid mass transfer measurements in a three-phase magneto fluidized bed, Chem. Eng. Sci. 52 (1997) 279–295.
[18] E. Sada, S. Katoh, M. Shiozawa, T. Fukui, Performance of fluidized bed reactors utilizing magnetic fields, Biotechnol. Bioeng. 23 (1981) 2561–2567.
[19] B.E. Terranova, M.A. Burns, Continuous cell suspension processing using magnetically stabilized fluidized beds, Biotechnol. Bioeng. 37 (1991) 110–120.
[20] D.J. Graves, Bioseparation in the magnetically stabilized bed, Chromatogr. Sci. 61 (1993) 187–207.
[21] V. Ivanova, J. Hristov, E. Dobreva, Z. Al-Qodah, I. Penchev, Performance of a magnetically stabilized bed reactor with immobilized yeast cells, Appl. Biochem. Biotechnol. 59 (2) (1996) 187–198.
[22] W. Colin, K. Kong, M. Gillian, W. Richard, M. Angel, C. Jorge, J. Eladia, G. Miguel, The magnetically stabilized fluidized bed bioreactor: a tool for improved mass transfer in immobilized enzyme systems, Chem. Eng. J. 61 (1996) 241–246.
[23] Z. Al-Qodah, Hydrodynamic behavior of magneto airlift column in a transverse magnetic field, Can. J. Chem. Eng. 78 (3) (2000) 1–10.
[24] Z. Al-Qodah, V. Ivanova, E. Dobreva, I. Penchev, J. Hristov, R. Petrov, Non-porous magnetic support for cell immobilization, J. Fermen. Bioeng. 72 (2) (1991) 114–119.
[25] Y. Sun, T. Nozawa, Sh. Furusaki, Gas holdup and volumetric oxygen transfer coefficient in a three-phase fluidized bed bioreactor, J. Chem. Eng. Jpn. 21 (1) (1988) 15–19.
[26] K. Okada, Y. Nagata, Y. Akagi, Effect of packed bed on mass transfer in external-loop airlift bubble column, J. Chem. Eng. Jpn. 29 (4) (1996) 582–587.
[27] S.D. Kim, C.G. Baker, M.A. Bergonou, Phase holdup characteristics of three-phase fluidized beds, Can. J. Chem. Eng. 53 (1975) 134–140.
[28] T. Chiv, M. Zeigler, Liquid holdup and heat transfer coefficient in liquid solid and three-phase fluidized beds, AIChE J. 31 (1985) 1504–1509.